Exhumation history of the Juhor Mts. in central Serbia, the Northern Serbo–Macedonian Subunit

Uros Stojadinovic, Hannah Pomella, Nemanja Krstekanić, Bojan Kostić, Maja Maleš, Nikola Randjelovic, Miloš Radonjić

Exhumation history of the Juhor Mts. in central Serbia, the Northern Serbo–Macedonian Subunit | Uros Stojadinovic, Hannah Pomella, Nemanja Krstekanić, Bojan Kostić, Maja Maleš, Nikola Randjelovic, Miloš Radonjić | Geologica Carpathica, Jun 2024 | 2024 | |

10.31577/GeolCarp.2024.12

http://dr.rgf.bg.ac.rs/s/repo/item/0008807

GEOLOGICA CARPATHICA, 2024, 75, 3, 213–223 https://doi.org/10.31577/GeolCarp.2024.12

Exhumation history of the Juhor Mts. in Central Serbia, the Northern Serbo–Macedonian Subunit

UROS STOJADINOVIC[1,✉], HANNAH POMELLA[2], NEMANJA KRSTEKANIĆ[1,3], BOJAN KOSTIĆ[1], MAJA MALEŠ[1,3], NIKOLA RANDJELOVIC[1,3] and MILOŠ RADONJIĆ[4]

[1]University of Belgrade, Faculty of Mining and Geology, Djušina 7, 11000 Belgrade, Serbia
[2]University of Innsbruck, Department of Geology, Innrain 52f, 6020 Innsbruck, Austria
[3]Utrecht University, Faculty of Geosciences, Princetonlaan 4, 3584CD Utrecht, The Netherlands
[4]Serbia ZiJin Mining, Čukaru Peki Mine, Geology Department, Suvaja 185A, 19210 Bor, Serbia

(Manuscript received March 31, 2024; accepted in revised form August 15, 2024; Associate Editor: Rastislav Vojtko)

Abstract: In this study, we combined low-t thermochronology with outcrop- to micro-scale kinematic and petrological observations in the metamorphic basement of the Juhor Mts. in Central Serbia. The Juhor Mts. comprise northern parts of the Europe-derived Serbo–Macedonian Unit, at the transition towards the Adria-derived tectonic units of the Internal Dinarides. The Late Paleozoic Variscan orogeny resulted in the medium-grade greenschist to amphibolite facies metamorphism in the core of the mountains, as inferred from our thin section-scale observations. During the subsequent Alpine orogeny, the tectonic setting of the entire Europe–Adria transitional area was strongly influenced by the geodynamic evolution of the intervening Neotethyan Vardar Ocean. The last recorded thermal overprint in the northern segments of the Serbo–Macedonian metamorphics occurred in the latest Jurassic due to their burial during the obduction of the Eastern Vardar ophiolites over the European continental margin. According to our thermochronological and field structural data, the exhumation of the Juhor Mts. metamorphic basement occurred during two separate phases of extensional deformations. During the Late Cretaceous extension, the Serbo–Macedonian metamorphics were exhumed for ~3 to 6 km along a ductile Morava shear zone, and later structurally juxtaposed against the low-grade metamorphics of the adjacent Supragetic Unit of the Serbian Carpathians. The latest phase of ~1 to 2,5 km tectonic exhumation and uplift in the Miocene took place along the brittle normal faults that accommodated the opening of the Morava Valley Corridor, which forms the southern prolongation of the Pannonian Basin. It is plausible, therefore, that these Miocene normal faults are reactivated segments of thrusts inherited from the preceding Paleogene phase of the Adria–Europe collision.

Keywords: Northern Serbo–Macedonian Subunit, low-t thermochronology, kinematic analyses, extensional deformations

Introduction

The Juhor Mts. in Central Serbia represent an inselberg of Paleozoic medium-grade metamorphic rocks surrounded by Miocene to Quaternary sediments of the Morava Valley Corridor, which forms the southern prolongation of the Pannonian Basin (Figs. 1, 2). The mountains are situated at the transition from the northeastern margin of the Dinarides orogen to the Serbian Carpathians. With the other uplifted areas along the western flank of the Morava Valley Corridor, the Juhor Mts. comprise the northern parts of the Serbo–Macedonian tectonic unit, which was structured during the Variscan orogeny (Dimitrijević 1997, Fig. 1b). During the Alpine orogeny, the Serbo–Macedonian Unit experienced complex, polyphase tectonic deformations associated with the geodynamic evolution of the northern branch of the Neotethys (or the Vardar Ocean, Dimitrijević 1997). This includes the latest Jurassic obduction of the Eastern Vardar Ophiolites (Schmid et al. 2008), followed by the Early Cretaceous contraction, the Late Cretaceous extension, and, once more, the contraction during the latest Cretaceous–Paleogene (Toljić et al. 2018; Stojadinovic et al. 2022; Stojadinovic & Krstekanić 2023). Furthermore, the northern segment of the Serbo–Macedonian Unit underwent strong, structural, and thermal overprint during the subsequent Oligocene–Miocene Pannonian Basin extension (the Northern Serbo–Macedonian Subunit, Stojadinovic et al. 2021 and references therein).

A sharp, morphological, stratigraphic, and petrological contrast between the Juhor Mts. metamorphics and the surrounding Miocene to Quaternary sediments indicates a strong tectonic omission along the flanks of the mountains. However, in such a complex setting, which is characterized by the switching of tectonic regimes, the tectonic exhumation mechanism is difficult to distinguish between contraction- and extension-driven. Therefore, the timing and styles of the Juhor Mts. tectonic uplift remain unclear. This study aims to quantify the timing, amounts, and mechanisms of the Juhor Mts. tectonic exhumation. For this purpose, coupled zircon and apatite fission track thermochronology was combined with field outcrop-scale to micro-scale kinematic

✉ corresponding author: Uros Stojadinovic
uros.stojadinovic@rgf.bg.ac.rs

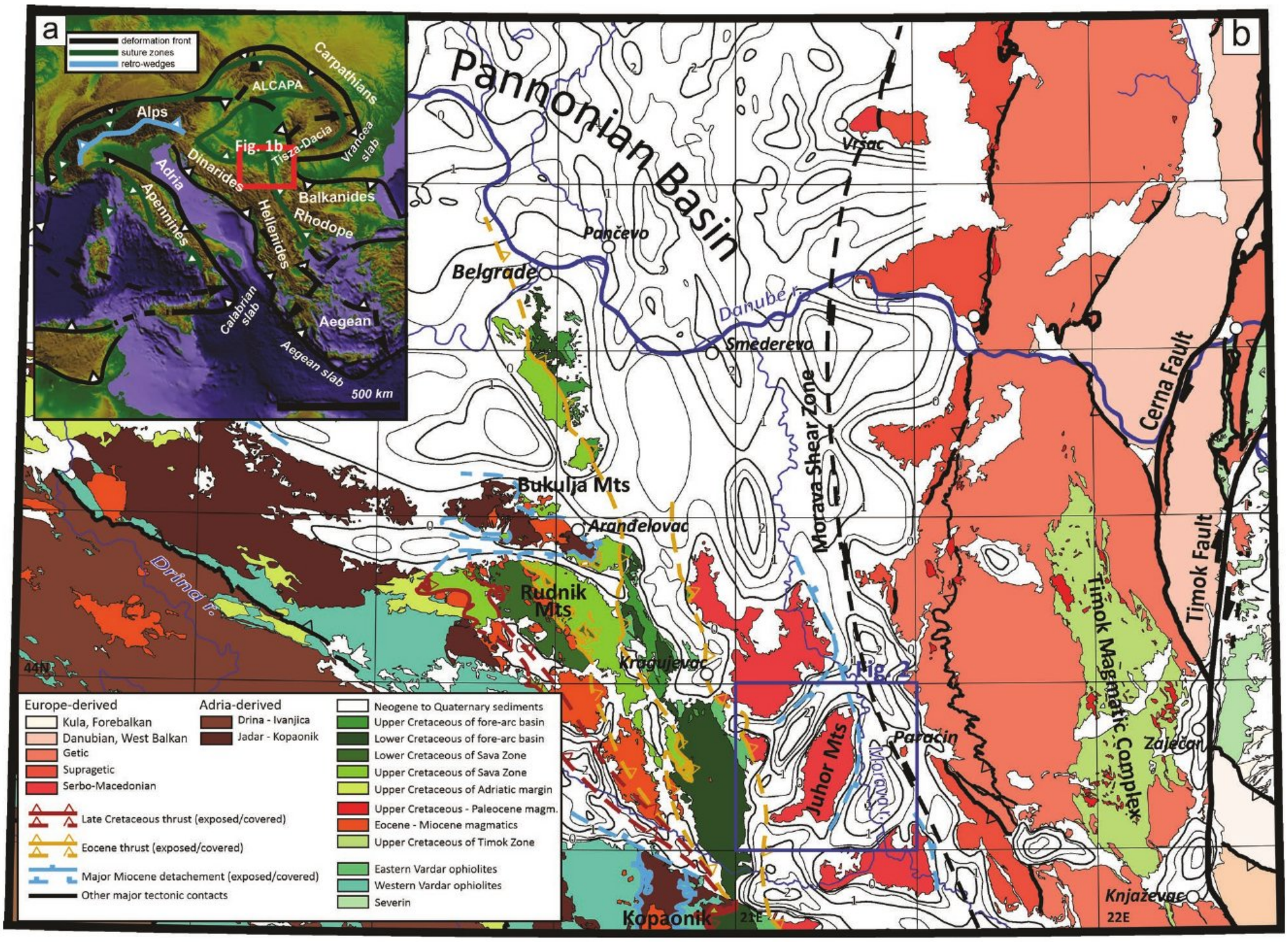

Fig. 1. a — Topographic map of Central Mediterranean orogens, displaying suture zones, orogenic fronts, and retro-wedges (modified after Krstekanić et al. 2020). The red rectangle marks the position of Fig. 1b; **b** — Geological map of the connection between the Dinarides, South Carpathians, and Pannonian Basin (modified after Stojadinovic et al. 2022). The blue rectangle indicates the location of the geological map in Fig. 2.

and petrological observations in the Juhor Mts. metamorphic basement. The obtained results thus allowed us to distinguish the Alpine tectonic events, which had a major impact on the present-day setting of the Dinarides–Carpathians transition area.

Tectono-stratigraphic evolution of the Serbo–Macedonian Unit

The Serbo–Macedonian Unit represents a belt of predominantly amphibolite facies metamorphic rocks, situated along the European continental margin, between the Pannonian Basin in the north and the Hellenides and Rhodope orogens in the south (Dimitrijević 1997, Fig. 1). Tectonically, it comprises the innermost parts of the Europe-derived Dacia tectonic Mega-Unit, juxtaposed against the Adria-derived units of the Internal Dinarides across the Adria-Europe collisional suture (i.e., the Sava Zone of Schmid et al. 2008). The Serbo–Macedonian Unit derives from a late Neoproterozoic–Silurian volcano-sedimentary complex, which underwent medium-grade metamorphism during the late Paleozoic Variscan orogeny (von Raumer et al. 2003; Antić et al. 2016a). During the Alpine orogeny, the tectonic setting of the Serbo–Macedonian Unit was strongly influenced by the geodynamic evolution of the northern branch of the Neotethys Ocean (or the Vardar Ocean, Dimitrijević 1997). The initial Triassic continental rifting in the Vardar Ocean separated Europe- from Adria-derived continental units, while its subsequent Jurassic–Cretaceous evolution structured the two continental margins. The Late Jurassic–Paleogene closure of the Vardar Ocean culminated in the latest Jurassic during the obduction-related thrusting of its eastern segments (the Eastern Vardar Ophiolitic Unit, Schmid et al. 2008) over the Triassic–Jurassic sedimentary cover of the Serbo–Macedonian metamorphics (see Maleš et al. 2023 and references therein). The Eastern Vardar ophiolites obduction led to the burial, which caused the youngest recorded latest Jurassic heating event in the medium-grade Serbo–Macedonian metamorphics in Central Serbia (Balogh et al. 1994). The ongoing Early Cretaceous convergence between the continental margins of Europe and Adria led to the E-ward subduction of the remaining Neotethys oceanic

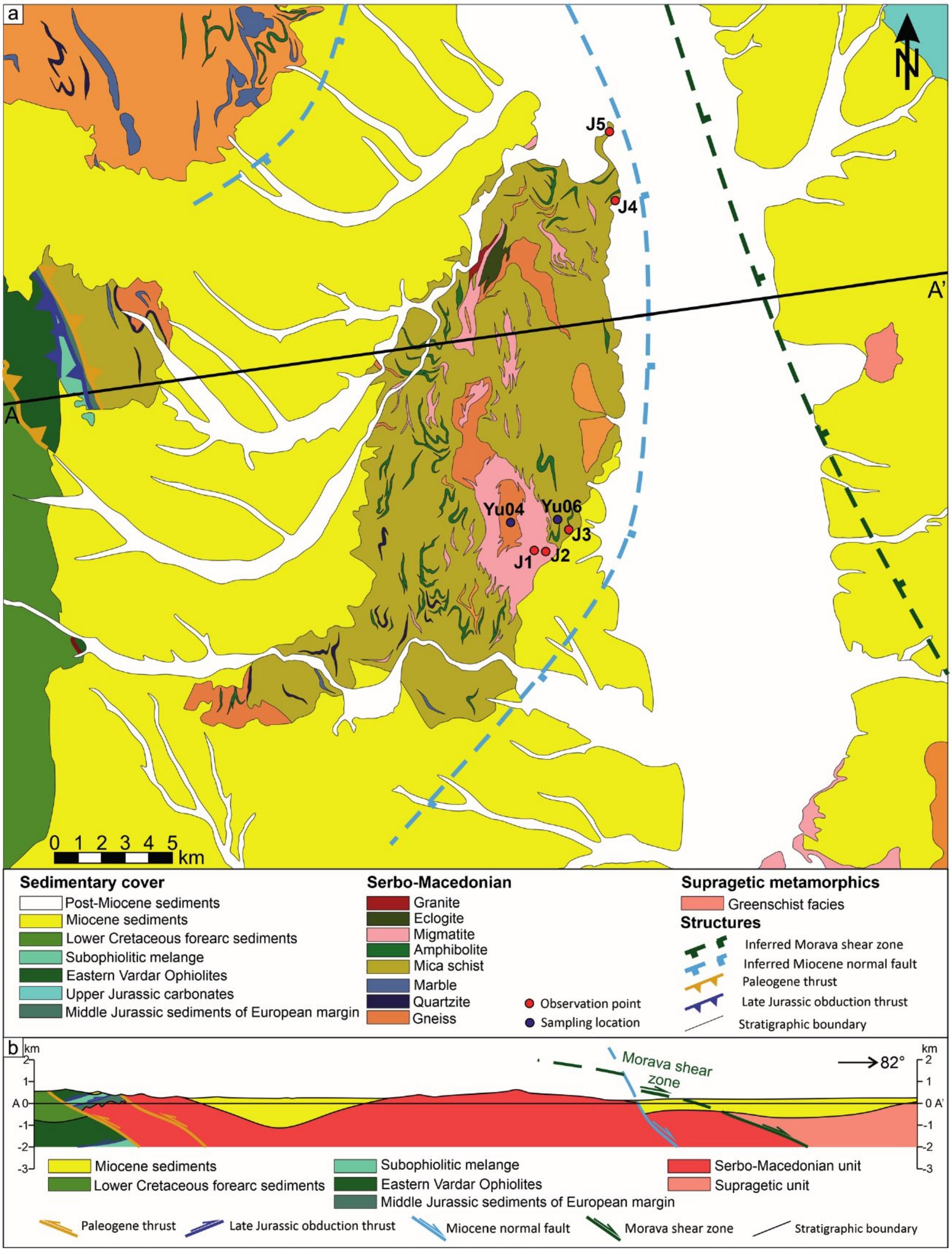

Fig. 2. a — Geological map of the Juhor Mts. (modified after the Basic geological map of former Yugoslavia scale 1:100,000, sheet Paraćin; Dolić et al. 1978); **b** — Simplified cross-section across the studied area. The cross-section location is indicated in Fig. 2a.

lithosphere beneath the active continental margin of the upper European plate (i.e., the Sava subduction system, Schmid et al. 2020). The roll-back and steepening of the subducting Neotethys oceanic lithosphere during the Late Cretaceous triggered the syn-subductional extension in the European upper plate domain of the Sava subduction system (Toljić et al. 2018, 2020). The Late Cretaceous extension structurally juxtaposed the medium-grade metamorphics of the Serbo–Macedonian Unit against the low-grade metamorphic rocks of the adjacent Supragetic Unit in the Serbian Carpathians (Antić et al. 2016b; Erak et al. 2017; Krstekanić et al. 2017; Stojadinovic et al. 2021). The extension occurred along the E-dipping ductile shear zone, which can be traced along the Serbo–Macedonian/Supragetic contact from the Vršac Mts. in the north, towards the southern termination of the Morava Valley Corridor in the south (i.e., the Morava shear zone, Fig. 1b). The latest Cretaceous–Paleogene collision thrusted Europe-derived continental units W-ward over the Late Cretaceous to Paleogene Sava trench turbidites and Adria-derived units of the Dinarides (Ustaszewski et al. 2010; Stojadinovic et al. 2022). The following Oligocene–Miocene extension affected the northern part of the Serbo–Macedonian Unit, causing the burial of large segments beneath the sediments of the southeastern Pannonian Basin (i.e., the Northern Serbo–Macedonian Subunit, Stojadinovic et al. 2021). The extension in the southeastern Pannonian Basin has a bi-directional orientation, which is the effect of the two retreating slabs, the Carpathian and Dinaridic (Matenco & Radivojević 2012). While the Dinaridic extension, oriented roughly E–W in the Morava Valley Corridor, had started previously during the Oligocene (see Andrić et al. 2018), the N–S oriented extension, controlled by the Carpathian slab-retreat, began in late Early Miocene times (Andrić et al. 2015; Balázs et al. 2016).

Geological setting of the Juhor Mts.

The core of the Juhor Mts. is comprised of Serbo–Macedonian Paleozoic medium-grade metamorphic rocks. The metamorphics are made up predominantly of amphibole-bearing orthogneisses, micaschists, and migmatites with intercalations of quartzites, as well as marbles. In the northwest part of the mountains, the metamorphics are intruded by a Paleozoic-age granitic body (Fig. 2, Dolić et al. 1978). Triassic to Jurassic sedimentary cover of the Serbo–Macedonian metamorphics is represented by scarce carbonates and clastics, which had undergone lower greenschist facies metamorphism during the obduction of the Eastern Vardar ophiolites in the latest Jurassic (Fig. 2, Maleš et al. 2023 and the references therein). The post-obductional overstep sedimentary sequence of the Eastern Vardar Ophiolitic Unit is represented by the Lower to Upper Cretaceous sediments deposited in a fore-arc basin along the European continental margin (see Toljić et al. 2018). The Neogene sedimentation in the Morava Valley Corridor begins with lower to middle Miocene continental alluvial to lacustrine deposits, which directly overlie the basement rocks (Sant et al. 2018). These are followed by transgressive middle Miocene (Badenian to Sarmatian) marine sediments (Fig. 2).

Methodological approach

The relationship between the exhumation processes acting in the Northern Serbo–Macedonian Subunit during the Alpine orogeny was studied by means of a low-temperature thermochronological study targeting exhumation below ~250 °C, including zircon fission-track (ZFT) and apatite fission-track (AFT), combined with field outcrop-scale to micro-scale kinematic observations.

Low-temperature thermochronology

Coupled zircon and apatite fission-track analyses were conducted on two rock samples in the Juhor Mts. Paleozoic-age metamorphic basement: Yu04 and Yu06 (Fig. 2). The sample Yu04 (coordinates 43°48’29” N, 21°15’32” E, altitude 710 meters) represents amphibole-bearing orthogneisses, while the sample Yu06 (coordinates 43°48’10” N, 21°17’56” E, altitude 260 meters) represents micaschists. An average of ~4 kg of rock was collected per each sampling location. Apatite and zircon mineral separation followed standard procedures, including crushing, sieving, heavy liquid, and magnetic separation. Samples were mounted in epoxy resin (apatite) and PFA® Teflon (zircon). Revelation of fossil tracks was achieved by etching polished zircon mounts for 8 h in a NaOH–KOH eutectic melt at 235 °C. Apatite mounts were etched in 5.5M HNO_3 at 21 °C for 20 s. Apatite and zircon grain mounts were dated by the external detector method (EDM; Gleadow & Duddy 1981), and irradiation of the mounts was performed at the Oregon State TRIGA reactor (USA). Induced tracks in external-detector muscovites were etched in 40 % HF for 45 min at 20 °C. Densities of spontaneous and induced tracks in zircon and apatite grains, as well as the track lengths in apatite, were determined using FT Studio Software V3 on an Autoscan® System (Autoscan System Ply. Ltd. 2002) with a Zeiss AxioImager M2m using a magnification of 1000×. Fission track ages are reported with statistical uncertainties, quoted at the ±2σ level, using a zeta factor of 229±21 (apatite, IRMM540 glass) and 178±6 (zircon, CN1 glass) (analyst Hannah Pomella). The obtained data were processed using the IsoplotR software (Vermeesch 2018). Horizontal confined track measurements, as well as the etch pit diameter (Dpar) measurements, were performed on the same apatite grain mounts. Time-temperature histories of the samples were modeled using HeFty software (Ketcham et al. 2003; Version 2.1.7. from 2023). Integrated AFT age data, track length distributions, and etch pit diameters (Dpar) were used as input parameters. ZFT central ages, including 2σ errors, were used as starting time-temperature boxes for the modelling. A second box covering the entire time-temperature range was used to ensure that the tested paths covered the entire

time-temperature space. The inverse Monte Carlo algorithm with the annealing model of Ketcham et al. (2007) was used for generating the time-temperature paths. The green envelopes represent 'acceptable' fits (merit value 0.05), while the pink ones represent 'good' fits (merit value 0.5) between the modeled and measured data. The black path in the Time-temperature model, as well as in the histogram, represents the best fit path. Zircon closure temperature was constrained to 250±50 °C, and zircon partial annealing zone (ZPAZ) to 300–200 °C (Tagami 2005). Apatite closure temperature was constrained to 110±10 °C, and apatite partial annealing zone (APAZ) to 120–60 °C (Gleadow & Duddy 1981). The present-day surface temperature was set to 20 °C. The fission track analytical data are reported in Tables 1 and 2, while sample locations are presented in Fig. 2a, and radial plots and time-temperature models are presented in Fig. 3.

Field structural observations and micro-scale analysis

We conducted fieldwork along the eastern flank of the Juhor Mts. to document the geometry of the outcrop-scale shear zones and other deformations, as well as take samples for thin-section analysis. At outcrops, foliation and shear zones dip direction/dip measurements were taken, and a very general sense of shear (i.e., tectonic transport) was documented wherever possible. In most situations, stretching lineations were not clear, and therefore, in such cases, a thin-section was taken parallel to the foliation dip. Thin-sections were analyzed by means of optical microscopy to obtain mineral assemblages, derive metamorphic grades, and observe micro-scale deformations.

Results

Apatite and zircon fission-track analyses

The orthogneiss sample Yu04 yielded a ZFT central age of 123.8±13.0 Ma (Table 2).

However, it must be noted that the ZFT single age distribution does not pass the Chi-squared test. The measured AFT central age of the same sample is 53.1±11.5 Ma, with a mean track length of 11.37±2.40 μm (26 tracks measured, Table 1). Thermal modelling of the sample Yu04 demonstrates its cooling from the upper limit of the ZPAZ to 70-90°C, which corresponds to the APAZ, during late Early Cretaceous to Late Cretaceous times (between ~130 Ma and 65 Ma, Fig. 3). However, the cooling path is not well-constrained for this part of the model. Between 65 Ma and 30 Ma the cooling path is well-constrained, and it indicates slow cooling to 60–80 °C. From 30 Ma to present times, the cooling rate has to speed up again, but the kink point is not clearly defined in the modelling results (Fig. 3).

The micaschists sample Yu06 yielded a ZFT central age of 108.5±10.7 Ma (Table 2). The AFT central age of the same sample is 43.5±9.6 Ma (does not pass the Chi-squared test), with a mean track length of 11.85±1.73 μm (29 tracks measured, Table 1). Thermal modelling of the sample Yu06 demonstrates its cooling from the upper limit of the ZPAZ to 70–90 °C, corresponding to the upper APAZ during late Early Cretaceous to Paleocene times (between ~110 Ma and 55 Ma, Fig. 3). Between 55 Ma and 20 Ma the cooling path, which is for this time step well-constrained, indicates slow cooling to 60–70 °C. From 20 Ma to present times, the cooling rate has to speed up again, but the kink point is not clearly defined in the modelling results. Nevertheless, based on the Tt-models, fast cooling seems to start a bit later in sample YU06, which is located at 450 meters lower altitude compared to sample YU04 (Fig. 3).

Outcrop-scale deformations

Field observations have shown that the foliation along the Eastern Juhor Mts. slopes dips mainly towards the east with moderate to high dip angles (Fig. 4a), while in the northernmost outcrops, foliation dips gently towards the NNW. This pervasive foliation often accommodates foliation-parallel slip in a generally eastward direction; however, due to the lack of

Table 1: Apatite fission-track data.

Sample	n	N_s	ρ_s	N_i	ρ_i	ρ_d	$P(\chi^2)$ (%)	Age (Ma)*	±2σ	Dpar (μm, mean)	±1σ	Length (n)	(μm, mean)	±1σ
YU04	38	536	2.427	939	4.253	8.173	96.72	53.1	11.5	1.57	0.18	26	11.37	2.40
YU06	33	769	5.063	1422	9.337	7.058	1.3	43.5	9.63	1.68	0.16	29	11.85	1.73

Note: Fission-track age is given as a central age. Samples were analysed dry with an Autoscan Trackscan Professional system at 1000× magnification, a zeta value of 229.64±21.8 (Hannah Pomella), a N_d value of 3000, and IRMM540 glass. ρ_S, $\rho_{i,}$ and ρ_d are given in e*10^5 tracks/cm^2

Table 2: Zircon fission-track data.

Sample	n	N_s	ρ_s	N_i	ρ_i	ρ_d	$P(\chi^2)$ (%)	Age (Ma)*	± 2σ
YU04	20	8877	112.5	3114	39.48	4.885	0.01	123.8	13.0
YU06	21	4531	113.9	1800	45.25	4.864	26.53	108.5	10.7

Note: Fission-track age is given as a central age. Samples were analysed dry with an Autoscan Trackscan Professional system at 1000× magnification, a zeta value of 178.38±6.25 (Hannah Pomella), a N_d value of 3200, and CN1 glass. ρ_S, ρ_i, and ρ_d are given in e*10^5 tracks/cm^2

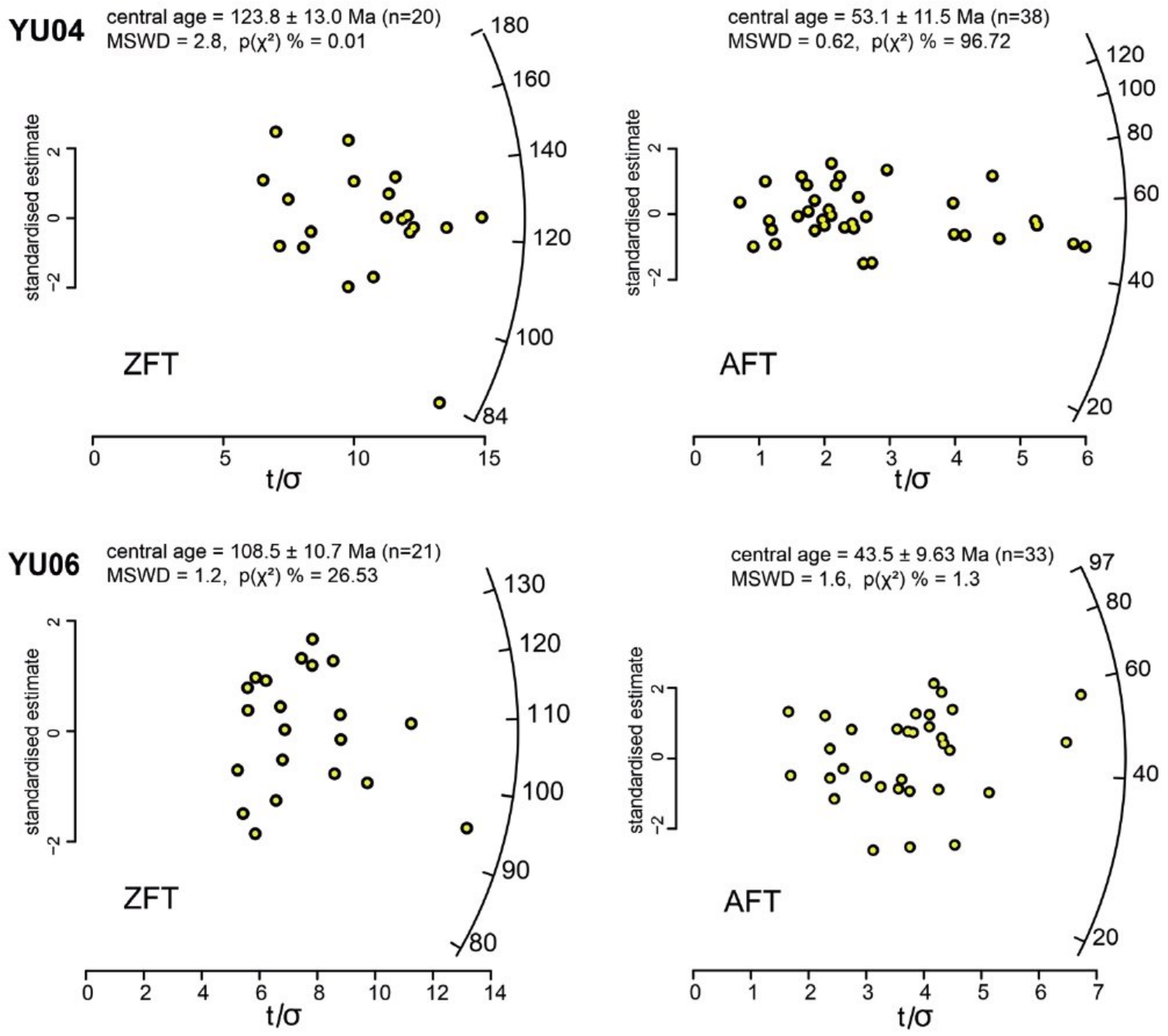
YU04
central age = 123.8 ± 13.0 Ma (n=20)
MSWD = 2.8, p(χ²) % = 0.01
standardised estimate
ZFT
t/σ
central age = 53.1 ± 11.5 Ma (n=38)
MSWD = 0.62, p(χ²) % = 96.72
AFT
YU06
central age = 108.5 ± 10.7 Ma (n=21)
MSWD = 1.2, p(χ²) % = 26.53
central age = 43.5 ± 9.63 Ma (n=33)
MSWD = 1.6, p(χ²) % = 1.3

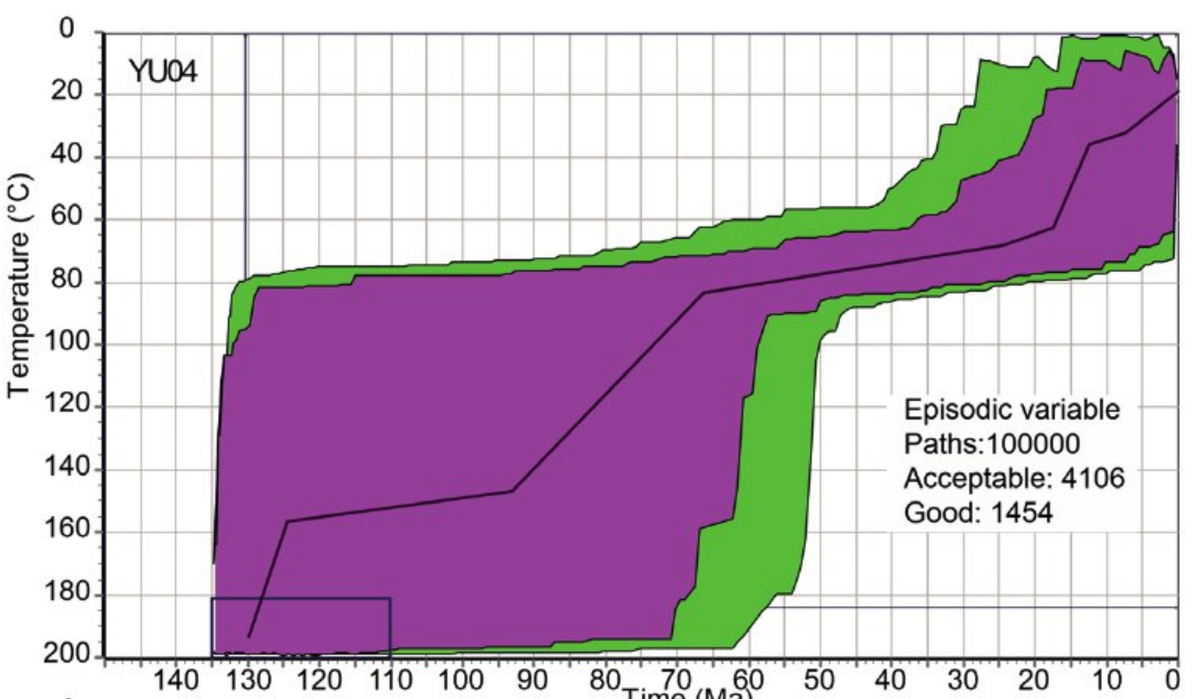
YU04
Temperature (°C)
Time (Ma)
Episodic variable
Paths:100000
Acceptable: 4106
Good: 1454
YU06
Episodic variable
Paths:100000
Acceptable: 2366
Good: 705

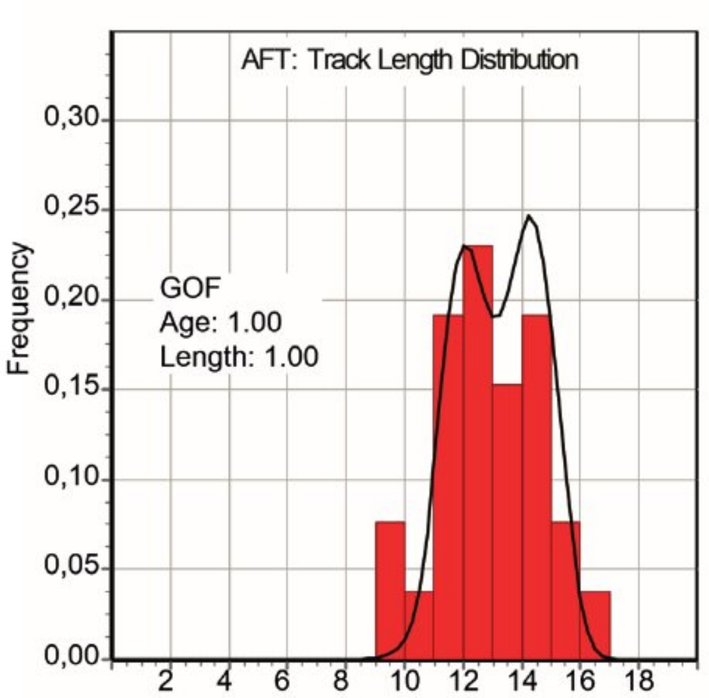
AFT: Track Length Distribution
Frequency
GOF
Age: 1.00
Length: 1.00
Length (μm)
AFT: Track Length Distribution
GOF
Age: 1.00
Length: 0.95
Length (μm)

Fig. 3. Low-t thermochronology of two metamorphic basement samples from the Juhor Mts. Locations of sampling sites are displayed in Fig. 2a. The radial plots in the top part of the figure that represent ZFT and AFT single grain age distributions were obtained using the IsoplotR (Vermeesch 2018). Abbreviations: n – number of grains counted; Ages are central ages; P – probability obtaining Chi-square (χ^2). Graphs in the bottom part of the figure represent the results of thermal modelling of AFT data of the two samples. Modelling was performed using the HeFty program (Ketcham et al. 2003; Version 2.1.7. from 2023). AFT age data, track length distributions, and etch pit diameters (D_{par}) were used as input parameters. ZFT central ages, including 2σ errors, were used as starting time-temperature boxes for the modelling. The green envelopes represent 'acceptable' fits (merit value 0.05), while the pink ones represent 'good' fits (merit value 0.5) between modeled and measured data. The black path in the Time-temperature model, as well as in the histogram, represents the best fit path. GOF=Goodness of fit.

clearly developed stretching lineation, it cannot be determined whether the tectonic transport is more towards NE or SE or anywhere in between. Locally, meter-scale overturned to recumbent isoclinal folds can be observed, indicating refolding of older deformation by ~eastward shearing (Fig. 4b). Statistical analysis of foliation dip direction/dip angle data obtained from the geological map (Basic Geological Map of SFRY, 1:100,000, sheet Paraćin) also demonstrates the dominant eastward dip of foliation with a maximum at 067/26 (Fig. 4c). However, there is significant variability of foliation orientation, both in terms of dip direction and dip angle, and a submaximum in 295/21 indicates refolding (Fig. 4c). In the vicinity of the contact between the Juhor Mts. metamorphic basement and the Miocene sediments of the Morava Valley Corridor, these ductile deformations were truncated by normal to oblique normal faults and associated Riedel shear structures that display eastward slip direction (Fig. 4d) and likely related to the Miocene extensional event.

Metamorphic grades and thin section-scale observations

Optical microscopy analysis has shown that the gneisses of the Juhor Mts. underwent a slightly lower grade metamorphism in the south (observation points J1-J3) compared to the north (observation points J4 and J5). It is important to note, however, that the two observations and sampling points in the north are located in the immediate vicinity of the Miocene normal fault. At the same time, the samples in the south were taken away from the contact with the Miocene sediments of the Morava Valley Corridor.

Thin-sections show that the dominant mineral assemblage in the south consists of quartz, plagioclase, orthoclase, microcline, muscovite, biotite, and locally garnet, while zircon and apatite are accessory minerals (Fig. 4e). Locally, biotite is weakly chloritized or retrogradely changed into magnetite. Quartz demonstrates undulose extinction and bulging as well as sub-grain rotation recrystallization, while perthite and antiperthite are common. Muscovite and biotite, together with elongated aggregates of quartz and feldspars, form a pervasive spaced foliation (Fig. 4e). The mineral assemblage and recrystallization features indicate greenschist facies metamorphism, with a temperature of 450–550 °C and pressure of 0.3–0.5 GPa.

In the north, the main rock-building mineral assemblage consists of quartz, plagioclase, muscovite, biotite, garnet, staurolite, kyanite, and orthoclase, but in less abundance than in the south (Fig. 4f). Accessory minerals are represented by zircon and apatite. Quartz displays undulose extinction and sub-grain rotation to grain boundary migration recrystallization, while garnet demonstrates retrograde changes within its corona made of chlorite, biotite, and quartz. Spaced foliation is pervasive, made of muscovite, biotite, and elongated quartz aggregates (Fig. 4f). Overall mineral assemblage and recrystallisation features demonstrate amphibolite facies metamorphism with a temperature of 500–600 °C and pressure of 0.4–0.6 GPa.

Interpretation and discussion

Modeled t–T histories indicate that the Juhor Mts. greenschist to amphibolite facies metamorphic basement underwent ~120 °C of cooling between late Early Cretaceous and Paleocene (between ~130 and 55 Ma, Fig. 3). During this lengthy interval, the upper tectonic plate of the Sava subduction/collision system was affected by two major phases of deformation: the Late Cretaceous extension and the latest Cretaceous to Paleogene contraction. According to existing structural and thermochronological studies, the upper plate of the Sava Zone could have recorded minor exhumation only during the very late stages of the Adria-Europe collision in the Late Eocene (not earlier than ~40 Ma, see Stojadinovic et al. 2017). Therefore, we suggest that the bulk of cooling in the Juhor Mts. metamorphics occurred during the Late Cretaceous syn-subductional extension in the upper European plate domain of the Sava subduction system (Toljić et al. 2018, 2020). The medium-grade Serbo–Macedonian metamorphics were exhumed below the low-grade metamorphics of the adjacent Supragetic Unit of the Serbian Carpathians along an E-dipping ductile shear zone (i.e., the Morava shear zone, Figs. 1b, 2b). The Morava shear zone belongs to the Late Cretaceous extensional faults system that had accommodated the exhumation of the Serbo–Macedonian metamorphic basement, coeval subsidence in the adjacent fore- and back-arc basins, and magmatism in the Timok Magmatic Complex (Fig. 5a). Given the cooling of ~120 °C and an estimated (paleo)geothermal gradient of ~30±10 °C/km, we can assume that the Late Cretaceous extension resulted in ~3 to 6 km of exhumation of the Serbo–Macedonian metamorphics.

According to the modelled t–T paths (Fig 3), following a phase of very slow cooling during the Eocene (between 55 and 30 Ma, Figs. 3, 5b), cooling rates speed up again from

~30 Ma onwards, leading to the final near-surface crustal cooling from ~ 80–60° to surface temperatures of the Juhor Mts. metamorphics (Fig. 3). We suggest that this final phase of cooling in the Juhor Mts. metamorphics occurred during the Oligocene–Miocene Pannonian Basin extension (Fig. 5c). The extension plausibly reactivated segments of thrusts inherited from the preceding Paleogene phase of the Adria–Europe collision, resulting in the opening of the Morava Valley Corridor. Given the high geothermal gradients during the Miocene (~40±10 °C/km, Adam & Wesztergom 2001; Lenkey

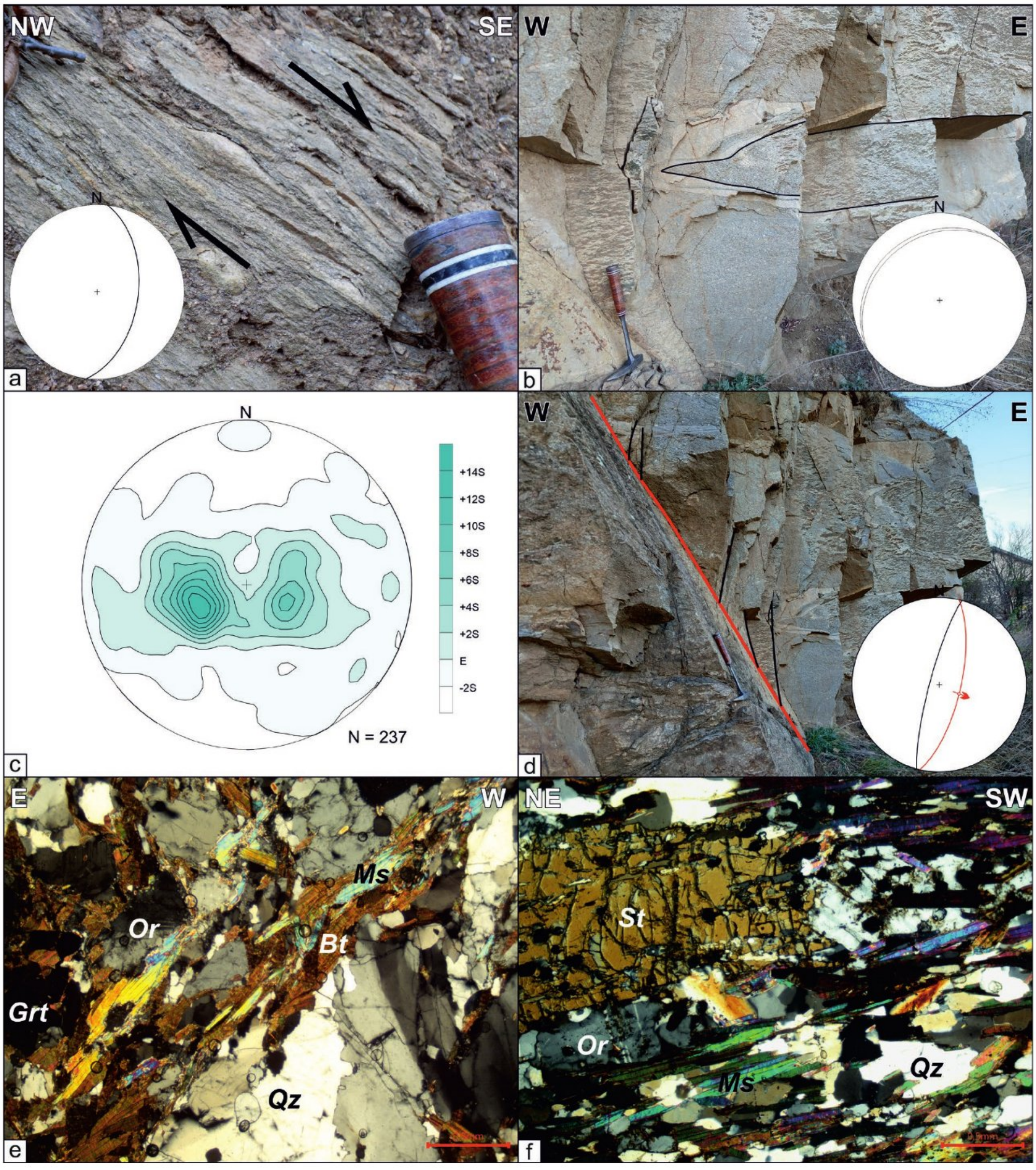

Fig. 4. Structures observed in outcrops and their stereonet projections (a, b, and d), statistical analysis of map data (c), and oriented thin-sections (e and f). Observation points are indicated in Fig. 2a. **a** — Ductile shear zone with ~top-E tectonic transport observed at point J2. **b** — Isoclinal fold observed at point J5. **c** — Statistical contour plot of foliation dip-direction/dip data documented on the Basic geological map of former Yugoslavia scale 1:100,000, sheet Paraćin (Dolić et al. 1978). **d** — Normal fault (red) with Riedel shears (black) observed at point J5. **e** — Thin-section of Juhor Mts. metamorphics collected at point J2. **f** — Thin-section of Juhor Mts. metamorphics collected at point J4.

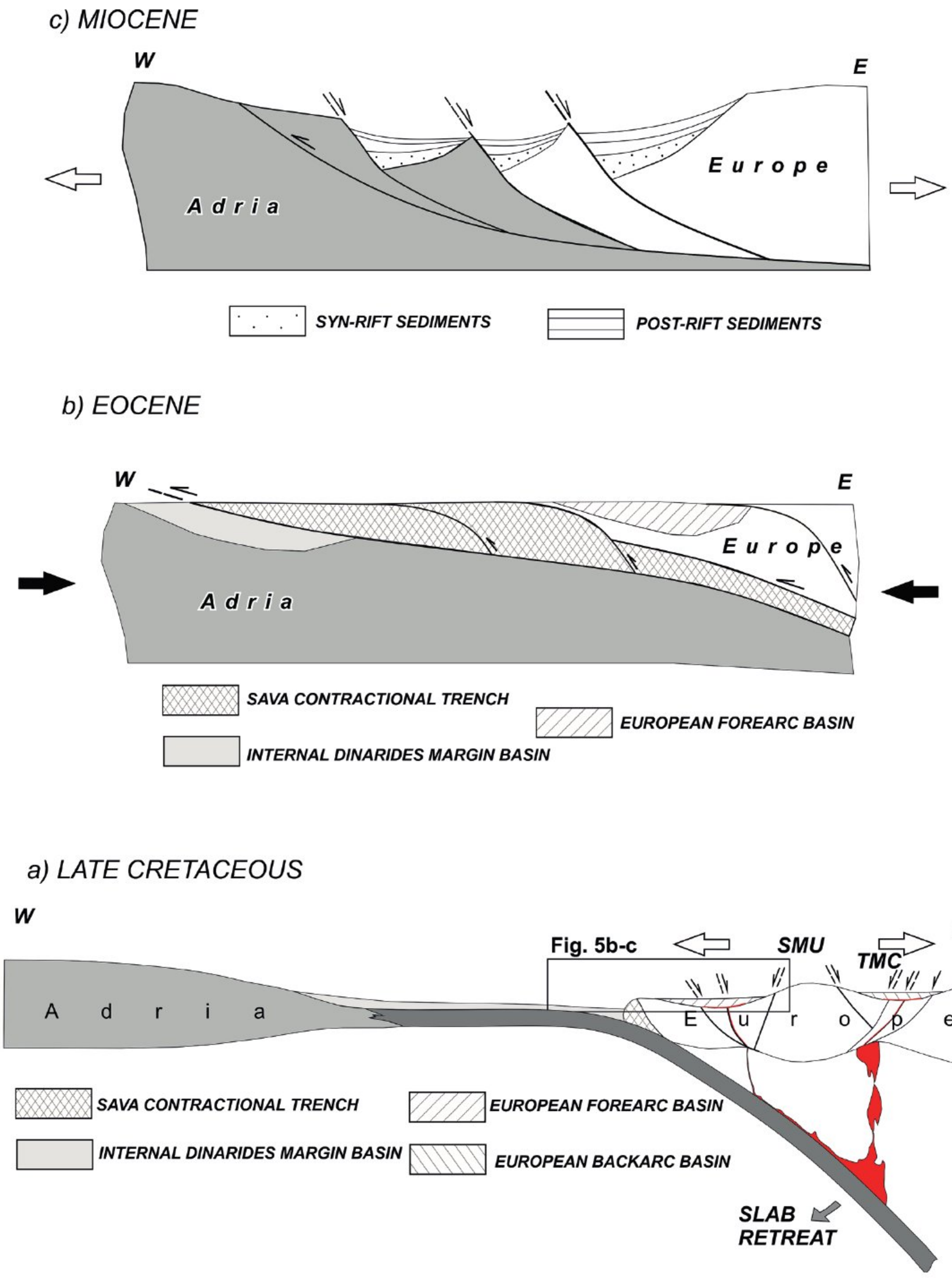

Fig. 5. Conceptual sketch (not to scale) of the Adria–Europe convergence zone evolution in central Serbia during Late Cretaceous–Miocene times (modified after Stojadinovic et al. 2017; Toljić et al. 2018, Stojadinovic & Krstekanić 2023). **a** — The Late Cretaceous extensional exhumation of the Serbo–Macedonian metamorphic basement (SMU) due to the Neotethyan slab rollback, associated with subsidence in the back-arc and fore-arc basins, partial melting, and magmatism in the Timok Magmatic Complex (TMC); **b** — Latest Cretaceous to Paleogene Adria–Europe continental collision, associated with W-ward thrusting of the Europe-derived continental units over the Sava trench turbidites and Adria-derived units of the Dinarides; **c** — Oligocene to Miocene Pannonian Basin extension.

et al. 2002), we estimate that the Pannonian Basin extension resulted in exhumation of the Serbo–Macedonian metamorphics of ~1 to 2.5 km. The maximum of 1–2.5 km Miocene tectonic uplift of the Juhor Mts. metamorphic basement, obtained by the thermal modelling, corresponds well with vertical offsets along the Miocene brittle normal faults recorded by syn-kinematic sedimentation observed in seismic cross-sections in the Morava Valley Corridor (Marović et al. 2007 and references therein).

Conclusions

The Juhor Mts. in Central Serbia keep a record of the complex tectonic evolution of the Serbo–Macedonian Unit. The Late Paleozoic Variscan orogeny resulted in the medium-grade greenschist to amphibolite facies metamorphism in the core of the Juhor Mountains, reaching ~450–600 °C and ~0.3–0.6 GPa, as inferred from our thin section-scale observations. The last recorded thermal overprint in the northern segments of the Serbo–Macedonian metamorphics occurred in the latest Jurassic due to their burial during the obduction of the Eastern Vardar ophiolites over the European continental margin. According to our thermochronological and field structural data, exhumation of the Juhor Mts. metamorphic basement occurred during two separate phases of extensional deformations. During the Late Cretaceous extension, the medium-grade metamorphics of the Serbo–Macedonian Unit were exhumed for ~3–6 km along a ductile Morava shear zone, and structurally juxtaposed against the low-grade metamorphics of the adjacent Supragetic Unit of the Serbian Carpathians. The latest phase of ~1 to 2.5 km tectonic exhumation and uplift in the Miocene took place along the brittle normal faults that accommodated the opening of the Morava Valley Corridor, the southern prolongation of the Pannonian Basin. These Miocene normal faults are plausibly reactivated segments of thrusts inherited from the preceding Paleogene phase of the Adria–Europe collision. Therefore, we can conclude that the bulk of exhumation of the Juhor Mts. metamorphics took place during two separate extensional phases: in the Late Cretaceous and in the Miocene. Contrarily, contractional deformations associated with the progressive closure of the Mesozoic Vardar Ocean predominantly led to the burial of the Serbo–Macedonian metamorphics.

Acknowledgments: This research was supported by the Science Fund of the Republic of Serbia, GRANT No TF C1389-YF, GEODYNAMICS OF BASINS ABOVE SUBDUCTED SLABS: an integrated modelling study of tectonics, sedimentation, and magmatism in the Timok Magmatic Complex – TMCmod (PROJECT No 7461).

References

Adam A. & Wesztergom V. 2001: An attempt to map the depth of the electrical asthenosphere by deep magnetotelluric measurements in the Pannonian basin (Hungary). *Acta Geologica Hungarica* 4, 167–192.

Andrić N., Fügenschuh B., Životić D. & Cvetković V. 2015: The thermal history of the Miocene Ibar Basin (Southern Serbia): New constraints from apatite and zircon fission track and vitrinite reflectance data. *Geologica Carpathica* 66, 37–50. https://doi.org/10.1515/geoca-2015-0009

Andrić N., Vogt K., Matenco L., Cvetković V., Cloetingh S. & Gerya T. 2018: Variability of orogenic magmatism during Mediterranean-style continental collisions: a numerical modelling approach. *Gondwana Research* 56, 119–134. https://doi.org/10.1016/j.gr.2017.12.007

Antić M., Peytcheva I., von Quadt A., Kounov A., Trivić B., Serafimovski T., Tasev G., Gerdjikov I. & Wetzel A. 2016a: Pre-Alpine evolution of a segment of the North-Gondwanan margin: Geochronological and geochemical evidence from the central Serbo–Macedonian Massif. *Gondwana Research* 36, 523–544. https://doi.org/10.1016/j.gr.2015.07.020

Antić M.D., Kounov A., Trivić B., Wetzel A., Peytcheva I. & Quadt A. 2016b: Alpine thermal events in the central Serbo–Macedonian Massif (southeastern Serbia). *International Journal of Earth Sciences* 105, 1485. https://doi.org/10.1007/s00531-015-1266-z

Balázs A., Matenco L., Magyar I., Horváth F. & Cloetingh S. 2016: The link between tectonics and sedimentation in back-arc basins: new genetic constraints from the analysis of the Pannonian Basin. *Tectonics* 35, 1526–1559. https://doi.org/10.1002/2015TC004109

Balogh K., Svingor E. & Cvetković V. 1994: Ages and intensities of metamorphic processes in the Batocina area, Serbo–Macedonian Massif. *Acta Mineralogica-Petrographica* XXXV, 81–94.

Dimitrijević M. D. 1997: Geology of Yugoslavia. *Geoinstitut-Barex*, Belgrade, 1–187.

Dolić D., Kalenić M., Lončarević Č. & Hadži-Vuković M. 1978: Osnovna geološka karta SFRJ 1:100.000. List Paraćin [Basic geological map of Former Yugoslavia 1:100,000. Sheet Paraćin]. Savezni Geološki zavod, Beograd (in Serbian).

Erak D., Matenco L., Toljić M., Stojadinović U., Andriessen P.A.M., Willingshofer E. & Ducea M.N. 2017: From nappe stacking to extensional detachments at the contact between the Carpathians and Dinarides – the Jastrebac Mountains of Central Serbia. *Tectonophysics* 710–711, 162–183. https://doi.org/10.1016/j.tecto.2016.12.022

Gleadow A.J.W. & Duddy I.R. 1981: A natural long-term track annealing experiment for apatite. *Nuclear Tracks* 5, 169–174. https://doi.org/10.1016/0191-278X(81)90039-1

Ketcham R.A., Donelick R.A. & Donelick M.B. 2003: AFT Solve: a program for multi-kinetic modeling of apatite fission-track data. *American Mineralogist* 88, 929–939.

Ketcham R.A., Carter A., Donelick R.A., Barbarand J., & Hurford A. J. 2007: Improved modeling of fission-track annealing in apatite. *American Mineralogist* 92, 799–810.

Krstekanić N., Stojadinović U., Kostić B. & Toljić M. 2017: Internal structure of the Supragetic Unit basement in the Serbian Carpathians and its significance for the late early cretaceous nappe-stacking. *Annales Geologiques de la Peninsule Balkanique* 78, 1–15.

Krstekanić N., Matenco L., Toljić M., Mandić O., Stojadinović U. & Willingshofer E. 2020: Understanding partitioning of deformation in highly arcuate orogenic systems: Inferences from the evolution of the Serbian Carpathians. *Global and Planetary Change* 195. https://doi.org/10.1016/j.gloplacha.2020.103361

Lenkey L., Dovenyi P., Horvath F. & Cloetingh S.A.P.L. 2002: Geothermics of the Pannonian basin and its bearing on the Neotectonics. *EGU Stephan Mueller Special Publication Series* 3, 29–40.

Maleš M., Randjelović N., Krstekanić N., Kostić B., Ćirić N. & Stojadinovic U. 2023: New insights into tectonic relations between the Eastern Vardar Ophiolites and Serbomacedonian Units: Inferences from a microtectonic study in central Serbia. *Annales Geologiques de la Peninsule Balkanique* 84, 33–45.

Marović M., Toljić M., Rundić Lj. & Milivojević J. 2007: Neoalpine Tectonics of Serbia. *Serbian Geological Society*, Belgrade.

Matenco L. & Radivojević D. 2012: On the formation and evolution of the Pannonian Basin: constraints derived from the structure of the junction area between the Carpathians and Dinarides. *Tectonics* 31, TC6007. https://doi.org/10.1029/2012TC003206

Sant K., Mandic O., Rundić Lj, Kuiper K.F. & Krijgsman W. 2018: Age and evolution of the Serbian Lake System: integrated results from Middle Miocene Lake Popovac. *Newsletters on Stratigraphy* 51, 117–143. https://doi.org/10.1127/nos/2016/0360

Schmid S.M., Bernoulli D., Fugenschuh B., Matenco L., Schefer S., Schuster R., Tischler M. & Ustaszewski K. 2008: The Alpine–Carpathian–Dinaridic orogenic system: correlation and evolution of tectonic units. *Swiss Journal of Geosciences*, 101, 139–183. https://doi.org/10.1007/s00015-008-1247-3

Schmid S.M., Fügenschuh B., Kounov A., Matenco L., Nievergelt P., Oberhansli R., Pleuger J., Schefer S., Schuster R., Tomljenović B., Ustaszewski K. & van Hinsbergen D.J.J. 2020: Tectonic units of the Alpine collision zone between Eastern Alps and western Turkey. *Gondwana Research* 78, 308–374. https://doi.org/10.1016/j.gr.2019.07.005

Stojadinovic U. & Krstekanić N. 2023: Tectono-sedimentary evolution of the NE Dinarides margin during the Cretaceous Adria–Europe convergence. *Annales Geologiques de la Peninsule Balkanique* 84, 65–74. https://doi.org/10.2298/GABP230112001S

Stojadinovic U., Matenco L., Andriessen P., Toljić M., Rundić L. & Ducea M.N. 2017: Structure and provenance of Late Cretaceous–Miocene sediments located near the NE Dinarides margin: inferences from kinematics of orogenic building and subsequent extensional collapse. *Tectonophysics* 710–711, 184–204. https://doi.org/10.1016/j.tecto.2016.12.021

Stojadinovic U., Krstekanić N., Kostić B., Ružić M. & Luković A. 2021: Tectonic evolution of the Vršac Mts. (NE Serbia): Inferences from field kinematic and microstructural investigations. *Geologica Carpathica* 72, 395–405. https://doi.org/10.31577/GeolCarp.72.5.3

Stojadinovic U., Krstekanić N., Matenco L. & Bogdanović T. 2022: Towards resolving Cretaceous to Miocene kinematics of the Adria–Europe contact zone in reconstructions: inferences from a structural study in a critical Dinarides area. *Terra Nova* 34, 523–534. https://doi.org/10.1111/ter.12618

Tagami T. 2005: Zircon fission-track thermochronology and applications to fault studies. Low temperature thermochronology: techniques, interpretations, and applications. *Reviews in Mineralogy and Geochemistry* 58, 95–122. https://doi.org/10.2138/rmg.2005.58.4

Toljić M., Matenco L., Stojadinović U., Willinshofer E. & Ljubović-Obradović D. 2018: Understanding fossil fore-arc basins: Inferences from the Cretaceous Adria–Europe convergence in the NE Dinarides. *Global and Planetary Change* 171, 167–184. https://doi.org/10.1016/j.gloplacha.2018.01.018

Toljić M., Trbić-Glavaš B., Stojadinovic U., Krstekanić N. & Srećković-Batoćanin D. 2020: Geodynamic interpretation of the Late Cretaceous syn-depositional magmatism in central Serbia: inferences from biostratigraphic and petrological investigations. *Geologica Carpatica* 71, 526–538. https://doi.org/10.31577/GeolCarp.71.6.4

Ustaszewski K., Kounov A., Schmid S.M., Schaltegger U., Krenn E., Frank W. & Fügenschuh B. 2010: Evolution of the Adria–Europe plate boundary in the northern Dinarides: from continent–continent collision to back-arc extension. *Tectonics* 29. https://doi.org/10.1029/2010TC002668

Vermeesch P. 2018: IsoplotR: A free and open toolbox for geochronology. *Geoscience Frontiers* 9, 1479–1493. https://doi.org/10.1016/j.gsf.2018.04.001

von Raumer J.F., Stampfli G.M. & Bussy F. 2003: Gondwana-derived microcontinents – the constituents of the Variscan and Alpine collisional orogens. *Tectonophysics* 365, 7–22. https://doi.org/10.1016/S0040-1951(03)00015-5